

**STUDY OF EFFECT OF POROSITY IN THE PRESENCE  
OF APPLIED MAGNETIC FIELD A COSINE FORM CONVEX CURVED PLATE MODEL**

**SYED ARISHIYA NASEEM FATIMA\*<sup>1</sup>, TRIMBAK BIRADAR<sup>2</sup>, S.T FATHIMA<sup>3</sup>  
AND HANUMAGOWDA B.N<sup>4</sup>**

<sup>1</sup>Department of Mathematics,  
K.C.T College of Engineering, Gulbarga-585104, India.

<sup>2</sup>Department of Mathematics,  
Sharnbasveshwar College of science, Gulbarga-585103.

<sup>3</sup>Ashford, West Monroe, Luisiana, USA-71291.

<sup>4</sup>Department of Mathematics, Reva University, Bangalore-560064, India.

*(Received On: 07-09-16; Revised & Accepted On: 30-09-16)*

---

**ABSTRACT**

*The study of effect of porosity in the presence of applied magnetic field is studied in case of cosine form convex curved plates. The magneto-hydrodynamic (MHD) Reynolds-type equation for convex curved plates is derived using the continuity equation and the MHD motion equations. According to the results obtained, the presence of applied magnetic field signifies an increase in the MHD pressure. Compared with the classical non-magnetic case, the magnetic-field effect characterized by the Hartmann number provides an enhancement to the MHD load-carrying capacity and the response time for the porous convex curved plates. It is observed that effect of porosity is to decrease the performance characteristics of the Cosine form convex curved plate model.*

**Keywords:** *convex curved plates, cosine function, porous medium, Magnetic field.*

---

**1. INTRODUCTION**

In recent years, the characteristic of Magneto-hydrodynamics (MHD) in flow analysis are important for many engineering and industrial applications. The MHD bearings with conducting fluids possess the high thermal-conductivity and high electrical-conductivity features over the conventional bearings [1-9]. The squeeze film lubrication for different configuration of bearings under the action of transverse magnetic field has been discussed by several authors [10-15]. Magneto hydrodynamic flow has many applications in aerodynamic heating, electrostatic precipitation, polymer technology, petroleum industry, accelerators, fluid droplets, MHD pumps, power generators and purification of crude oil. Flow through porous medium has numerous engineering and geophysical applications.

Self-lubricating porous bearings have been studied in the last few decades because of their industrial applications and machine manufacturing. These bearings have self-contained oil reservoir and hence do not require continuous lubrication. Most porous bearings have interconnecting pores which store the lubricating fluid. When the normal load is applied, the fluid is supplied through the interconnected pores to the fluid film region to support the load, and when the load is removed from the loaded zone of the bearing, fluid is reabsorbed by capillary action. Since these can operate without additional lubricant for longer period, porous bearings have been used widely, where re-lubrication would be difficult. Thus, porous metal bearings have been used in the manufacturing of vehicles, home appliances, machines, and so forth. Because of the importance of porous bearings, Wu [16] studied the squeeze film effects between two rectangular plates in which both plates have a porous material. Numerous papers are available in the literature for the study of different types of porous bearings for example, journal bearings [17], slider bearings [18], thrust bearings [19], and many more.

---

**Corresponding Author: Syed Arishiya Naseem Fatima\*<sup>1</sup>**

**<sup>1</sup>Department of Mathematics, K.C.T College of Engineering, Gulbarga-585104, India.**

The study of porosity in the presence of applied magnetic field considering cosine form convex curved plate model has not been studied so far. Hence, in this paper an attempt has been made to study the effect of porosity in the presence of applied magnetic field in case of Cosine form convex curved plates. Modified Reynolds equation is obtained using Darcy's law for porous media and expressions for the MHD pressure, load carrying capacity and the time height relation are obtained.

## 2. MATHEMATICAL FORMULATION OF THE PROBLEM

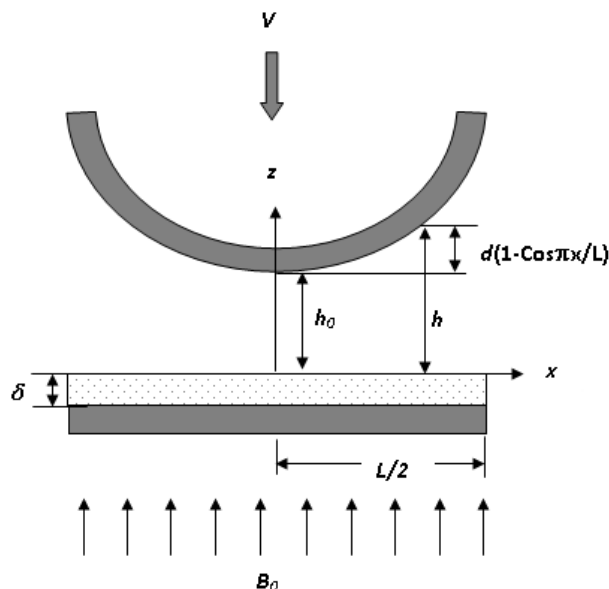


**Figure-1:** The physical configuration of convex curved - plates mode in the presence of transverse magnetic field.

Figure.1 shows the squeeze film geometry between the cosine form convex curved plates. The lower plate with a porous facing of thickness  $\delta$  is fixed and the upper plate has a squeezing velocity  $\left(\frac{dh}{dt}\right)$  is approaching the lower plate under a constant load. The film thickness  $h$  for the squeeze film can be generated by the form of a cosine function  $h = h_0 + d \left\{ 1 - \cos\left(\frac{\pi}{L}x\right) \right\}$ . In the equation,  $L$  is the length of the plates,  $d$  is the amplitude of the cosine function, and  $h_0$  is the minimum film thickness. At the central position:  $x = 0$ , the film thickness is equal to the minimum film thickness  $h_0$ . At the edge position:  $x = \frac{L}{2}$ , the film thickness is equal to the sum of the minimum film thickness and the amplitude  $h_0 + d$ . A uniform transverse magnetic field  $B_0$  is applied to the bearing in the  $z$  - direction as shown in the above figure1. It is assumed that the fluid film is thin, the body forces and the body couples are negligible. Under these assumptions, the hydrodynamic lubrication theory applicable to thin films, the continuity equation and the MHD governing equations of motion in rectangular coordinate are

$$\frac{\partial^2 u}{\partial z^2} - \frac{M_0^2}{h_0^2} u = \frac{1}{\mu} \frac{\partial p}{\partial x} \quad (1)$$

$$\frac{\partial p}{\partial z} = 0 \quad (2)$$

$$\frac{\partial u}{\partial x} + \frac{\partial w}{\partial z} = 0 \quad (3)$$

Where  $M = \frac{M_0}{h_0}$  and  $M_0 = B_0 h_0 \left(\frac{\sigma}{\mu}\right)^{1/2}$  is the Hartmann number.

The relevant boundary conditions for the velocity components are

i) At the upper surface  $z = h$

$$u = 0 \text{ (no Slip)} \quad w = V = dh/dt \text{ (Squeezing Velocity)} \quad (4)$$

ii) At the lower surface  $z = 0$

$$u = 0 \text{ (no Slip)} \quad w = w^* \tag{5}$$

Where  $w^*$  is the modified Darcy velocity component in the  $z$  – direction in the porous region. Modified form of the Darcy law for porous material is given by

$$u^* = -\frac{k}{\mu} \frac{\partial p^*}{\left(1 + \frac{kM_0^2}{mh_0^2}\right) \partial x} \tag{6}$$

$$w^* = -\frac{k}{\mu} \frac{\partial p^*}{\partial z} \tag{7}$$

Where  $k$  is the permeability of porous matrix,  $m$  porosity and  $p^*$  is the pressure in the porous region.

The solution of equation (1) subject to the boundary conditions eqns. (4) and (5) is given by

$$u = \frac{1}{\mu M^2} \frac{\partial p}{\partial x} \left( \frac{2 \sinh \frac{Mz}{2} \sinh \frac{M(z-h)}{2}}{\cosh \frac{Mh}{2}} \right) \tag{8}$$

Substituting above value of  $u$  in the integral form of continuity equation:

$$\frac{\partial}{\partial x} \left\{ \int_0^h u dz \right\} + w_h - w_0 = 0 \tag{9}$$

Substituting equations (6) and (7) in the following continuity equation for lower porous region

$$\frac{\partial u^*}{\partial x} + \frac{\partial w^*}{\partial z} = 0 \tag{10}$$

Integrating above equation once with respect to  $z$  from  $-\delta$  to  $0$  and using the Morgan-Cameron approximation with the condition  $\partial p^* / \partial z = 0$  when  $z = -\delta$  gives

$$\left( \frac{\partial p^*}{\partial z} \right)_{z=0} = -\frac{\delta}{c^2} \frac{\partial^2 p}{\partial x^2} \tag{11}$$

where  $c^2 = \left(1 + \frac{kM_0^2}{mh_0^2}\right)$  and  $\delta$  is the thickness of the porous layer.

Substituting (8) and (11) in (9) gives

$$\frac{\partial}{\partial x} \left\{ \frac{1}{\mu M^3} \frac{\partial p}{\partial x} \left( Mh - 2 \tanh \frac{Mh}{2} \right) + \frac{k\delta}{\mu c^2} \frac{\partial p}{\partial x} \right\} = -V \tag{12}$$

Introducing the dimensionless quantities

$$x^* = \frac{x}{L}, h^* = \frac{h}{h_0}, P^* = -\frac{ph_0^3}{\mu L^2 (dh/dt)}, A = \frac{d}{h_0}, \psi = \frac{k\delta}{h_0^3}, \delta^* = \frac{\delta}{h_0}$$

Equation (12) takes the form

$$\frac{\partial}{\partial x^*} \left\{ \frac{\partial P^*}{\partial x^*} F(h^*, M_0, \psi) \right\} = -1 \tag{13}$$

Where  $F(h^*, M_0, \psi) = \frac{1}{M_0^3} \left( M_0 h^* - 2 \tanh \frac{M_0 h^*}{2} \right) + \frac{\psi}{C^2}$ ,

$$C^2 = \left(1 + \frac{\psi M_0^2}{m\delta^*}\right) \text{ and } h^* = 1 + A \{1 - \cos(\pi x^*)\}.$$

The pressure conditions are:  $P^* = 0$  at  $x^* = \pm \frac{1}{2}$  and  $\frac{dP^*}{dx^*} = 0$  at  $x^* = 0$ .

Integrating (13) and using the pressure conditions, one can obtain

$$P^* = - \int_{1/2}^{x^*} \frac{x^*}{F(h^*, M_0, \psi)} dx^*$$

$$P^* = \int_{x^*}^{1/2} \frac{x^*}{F(h^*, M_0, \psi)} dx^* \quad (14)$$

Integrating the film pressure, one can obtain the load-carrying capacity

$$W = b \int_{-L/2}^{L/2} p dx \quad (15)$$

Where  $b$  denotes the width of the curved plates. Introducing a non-dimensional form gives

$$W^* = \frac{h_0^3 W}{\mu L^3 b (-dh/dt)} = \int_{-1/2}^{1/2} P^* dx^* \quad (16)$$

After performing the integration, one can obtain the non-dimensional load capacity.

$$W^* = \int_{-1/2}^{1/2} \left\{ \int_{x^*}^{1/2} \frac{x^*}{F(h^*, M_0, \psi)} dx^* \right\} dx^* \quad (17)$$

Introducing non-dimensional time as:

$$T^* = \frac{Wh_0^2 t}{\mu L^3 b} \quad (18)$$

The elapsed time required for the upper curved plate to approach the lower plate is given by

$$T^* = \int_{h_0^*}^1 \left[ \int_{-1/2}^{1/2} \left\{ \int_{x^*}^{1/2} \frac{x^*}{F(h^*, M_0, \psi)} dx^* \right\} dx^* \right] dh_0^* \quad (19)$$

for  $T^*, h^* = h_0^* + A \{1 - \cos(\pi x^*)\}$ .

Using the numerical method of integration, the film pressure (14), the load capacity (17) and the elapsed time (19) can be calculated.

### 3. RESULTS AND DISCUSSIONS

The effect of porosity on cosine form convex curved plates in the presence of magnetic field is observed and the squeeze film characteristics are analysed with respect to the non-dimensional parameters namely the Hartmann number  $M_0$  and permeability parameter  $\psi$ . All required characteristic features of squeeze film bearings such as the pressure distribution, load-carrying capacity, and squeezing time have been obtained as functions of dimensionless Hartmann number  $M_0$  and permeability parameter  $\psi$ .

#### 3.1. Squeeze film pressure

Figure 2, 3 represents the variation of non-dimensional pressure  $P^*$  with horizontal coordinate  $x^*$  for different values of  $\psi$  and  $M_0$ . These figures show the effect of magnetic field in terms of pressure distribution when other parameters are held fixed. It is observed that the pressure distribution increases for increasing values of  $M_0$  compared to nonmagnetic field ( $M_0 = 0$ ). An increase in the values of  $M_0$  makes lubricant to acquire more magnetization which in turn interacts with the magnetic field imposed. Also applied magnetic field normal to the flow reduces the velocity of the fluid in the film region which retains substantial amount of fluid. This fluid generates the pressure distribution.

### 3.2. Load carrying capacity

Figure 4, 5 shows the variation of non-dimensional  $W^*$  with amplitude ratio  $A$  for different values of  $\psi$  and  $M_0$ . It is clearly observed from this figure that the load capacity increases for increasing magnetic number compared to  $M_0 = 0$ . For increasing values of  $M_0$ , pressure distribution increases in the fluid region, hence, load capacity also increases. The effects are more distinct in convex curved plates in presence of transverse magnetic field. The increase in  $W^*$  is more evident for larger values of  $M_0$ .

### 3.3. Non-dimensional Squeeze film time

Figure 6, 7, 8 represents Variation of non-dimensional squeeze film time  $T^*$  with  $h_0^*$  for different values of  $M_0$  and  $\psi$ . The response times of convex curved porous squeeze films are significantly extended in the presence of external magnetic field. As magnetic parameter increases, the squeeze film time also increases. The applied magnetic field strongly opposes the fluid flow in the film region which retains large number of fluid in the film region. Thus, there is significant increase in squeezing time.

Table.1-Illustrates the effect of transverse magnetic field on the squeeze film characteristics, and is evaluated by the relative percentage difference. The relative variation of load capacity and the approaching time of porous convex curved squeeze films is tabulated, and it is observed that the performance characteristics are improved for higher values of magnetic parameter  $M_0$ . The increase in the non-dimensional load carrying capacity  $R_{W^*}$  and non-dimensional

squeeze film time  $R_{T^*}$  are defined by  $R_{W^*} = \left\{ \left( W_{magnetic}^* - W_{non-magnetic}^* \right) / W_{non-magnetic}^* \right\} \times 100$

And  $R_{T^*} = \left\{ \left( T_{magnetic}^* - T_{non-magnetic}^* \right) / T_{non-magnetic}^* \right\} \times 100$

The values of  $R_{W^*}$  and  $R_{T^*}$  are listed in Table. 1 for various values of  $M_0$  and  $\psi$ .

## 4. CONCLUSION

The study of effect of porosity on the performance characteristics of cosine form convex curved plates in the presence of magnetic field is studied. The squeeze film characteristics for porous convex curved plates are improved in presence of external magnetic fields i.e, the load carrying capacity and squeeze film time increases for increasing values of magnetic parameter  $M_0$ . It is observed that the pressure distribution, load-carrying capacity, and squeeze time increases for increasing values of Hartmann number, It is observed that effect of porosity on the permeability of cosine form convex curved is found to decrease these effects.

### Nomenclature:

- $B_0$  applied magnetic field in the  $z$ -direction
- $L$  length of the plates
- $d$  amplitude of the cosine function
- $b$  width of the curved plates
- $A$  amplitude ratio of the cosine-form convex curved plates
- $h_0$  minimum film thickness
- $h_0^*$  dimensionless film thickness after time  $\Delta t$
- $k$  permeability of the porous matrix
- $p$  hydrodynamic film pressure
- $p^*$  pressure in the porous region
- $M_0$  Magnetic Parameter  $\left( = B_0 h_0 \left( \frac{\sigma}{\mu} \right)^{1/2} \right)$
- $u, v$  Velocity components in film region
- $u^*, w^*$  Velocity components in porous region

$x, z$	local Cartesian co-ordinates
$m$	porosity
$P^*$	dimensionless pressure $\left( = \frac{ph_0^3}{\mu L^2 (-dh/dt)} \right)$
$t$	mean time of approach
$T^*$	Dimensionless time of approach $\left( = \frac{h_0^2 W t}{\mu L^3 b} \right)$
$V$	Squeezing Velocity $\left( -\frac{dh}{dt} \right)$
$W^*$	Dimensionless load carrying capacity $\left( = \frac{h_0^3 W}{\mu L^3 b (-dh/dt)} \right)$

### Greek symbols

$\sigma$	Conductivity of fluid
$\psi$	nondimensional permeability parameter
$\delta$	thickness of the porous layer
$\delta^*$	dimensionless thickness of the porous layer
$\mu$	lubricant viscosity

### REFERENCES

- [1]. Hays, D.F., "Squeeze Films for Rectangular Plates," ASME Journal of Basic Engineering, Vol. 85, (1963), pp. 243-246.
- [2]. Murti, P.R.K., "Squeeze Films in Curved Circular Plates," ASME Journal of Lubrication Technology, Vol. 97, (1975), pp. 650-652.
- [3]. Pinkus, O., and Sternlicht, B., Theory of Hydrodynamic Lubrication, McGraw Hill, New York (1961).
- [4]. Lin, J.R., "Pure Squeeze Film Behavior in a Hemispherical Porous Bearing Using the Brinkman Model," STLE Tribology Transactions, Vol. 39, (1996), pp. 769-778.
- [5]. Hamrock, B.J., Fundamentals of Fluid Film Lubrication, McGraw-Hill, New York (1994).
- [6]. Lin, J.R., Liao, W.H. and Hung, C.R., "The Effects of Couple Stresses in the Squeeze Film Characteristics between a Cylinder and a Plane Surface," Journal of Marine Science and Technology, Vol. 12, (2004), pp. 119-123.
- [7]. Lin, J.R., "Squeeze Film Characteristics between a Sphere and a Flat Plate: Couple Stress Fluid Model," Computers and Structures, Vol. 75, (2000), pp. 73-80.
- [8]. Barus, C., "Isothermals, Iopiestic, and Iometrics Rlative to Viscosity," American Journal of Science, Vol. 45,(1893), pp. 87-96.
- [9]. Lu, R.F. and Lin, J.R., "A Theoretical Study of Combined Effects of Non Newtonian Rheology and Viscosity-pressure Dependence in the Sphere-plate Squeeze-film system," Tribology International, Vol. 40, (2007), pp. 125-131.
- [10]. W.F.Hughes, "The magnetohydrodynamic Finite Step Slider bearing," Journal of fluids engineering, Trans. ASME, series D, vol.85, no.1, (1963), pp.129-135.
- [11]. W. F. Hughes and R. A. Elco, "MHD lubrication flow between parallel rotating disks, "Journal of Fluid Mechanics, vol. 13, no.1,(1962), pp. 21-32.
- [12]. D.C. Huzma, "The Magneto-hydrodynamic parallel slider bearing," Journal of Fluids engineering, Trans. ASME, series D, vol.87, (1965), pp.778-780.
- [13]. D. C.Kuzma, E. R. Maki ,and R. J.Donnely, "The MHD squeeze film," Journal of Fluid Mechanics, vol.19, no. 3, (1964), pp. 395-400.
- [14]. W. F.Huges and R.J. Elco, "Magneto-hydrodynamic journal bearing," Journal of American Rocket society, vol.32, (1962), pp.776-778.
- [15]. J. R .Lin, "Magneto-hydrodynamic squeeze film characteristics between annular plates," Industrial Lubrication and Tribology, Vol. 53, no. 2, (2001), pp.66 - 71.
- [16]. H.Wu, "Analysis of the squeeze film between porous rectangular plates," Journal of Lubrication Technology, vol. 94, no. 1, (1972), pp. 64-68.
- [17]. J. Prakash and S. K. Vij, "Load capacity and time-height relations for squeeze films between porous plates," Wear, vol. 24, no. 3, (1973), pp. 309-322.

[18].U. Srinivasan, "The analysis of a double-layered porous slider bearing," Wear, vol.42, no. 2, (1977), pp. 205–215.  
 [19].R. S. Gupta and V. K. Kapur, "Centrifugal effects in hydrostatic porous thrust bearings," Journal of Lubrication Technology, vol. 101, no. 3, (1979), pp. 381– 392.

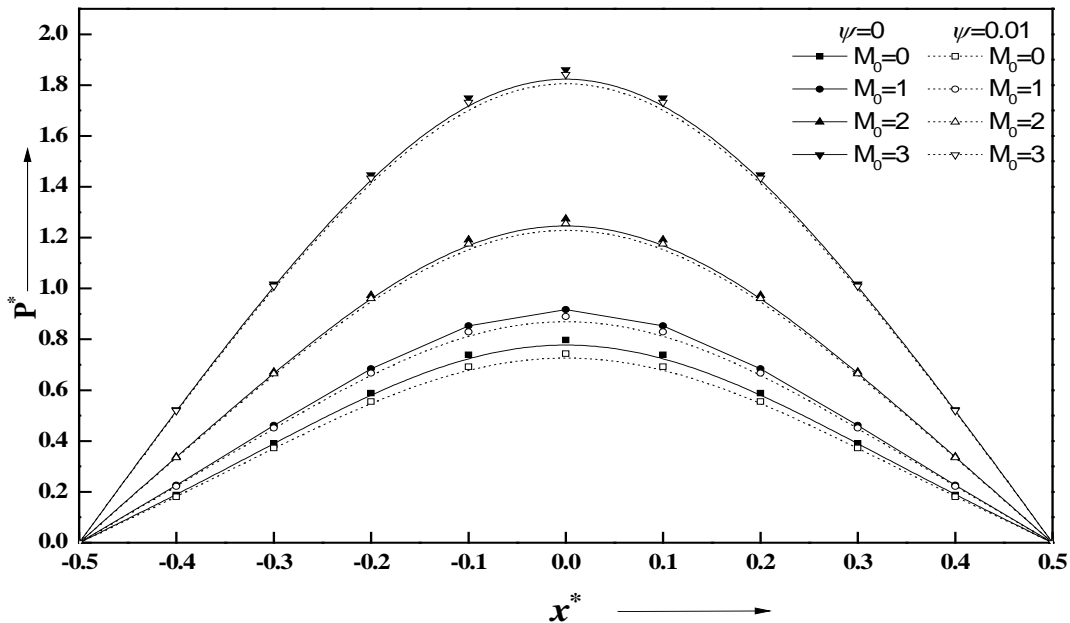


Fig.2 Variation of non-dimensional  $P^*$  with  $x^*$  for different values of  $\psi$  and  $M_0$  with  $\delta=0.01$

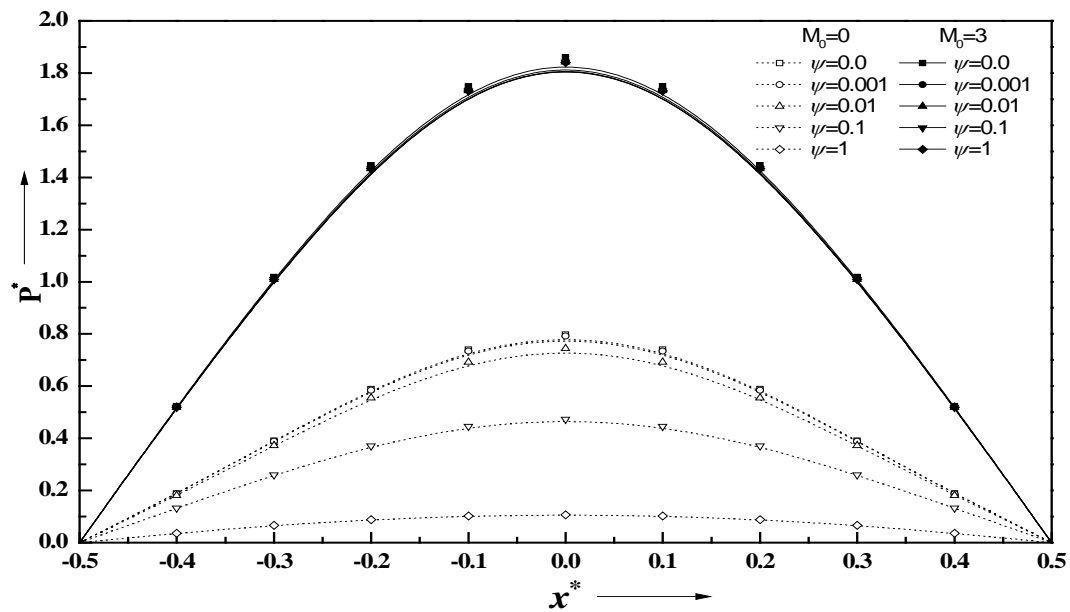


Fig.3 Variation of non-dimensional  $P^*$  with  $x^*$  for different values of  $\psi$  and  $M_0$  with  $\delta=0.01$

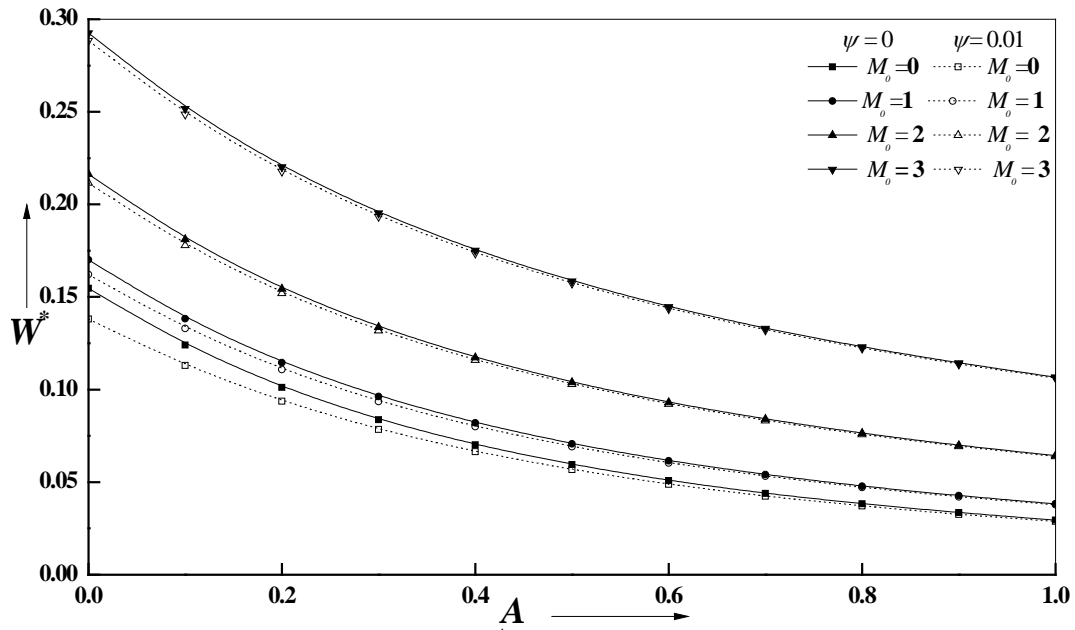


Fig. 4 Variation of non-dimensional  $W^*$  with amplitude ratio  $A$  for different values of  $\psi$  and  $M_0$ .

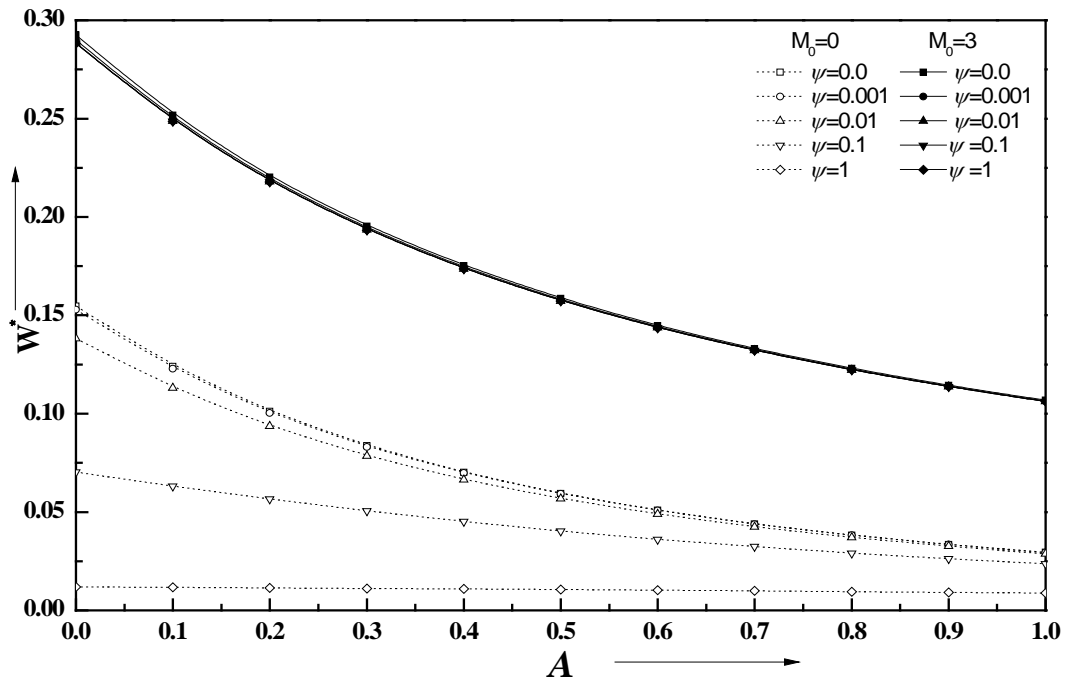


Fig.5 Variation of non-dimensional  $W^*$  with  $A$  for different values of  $\psi$  and  $M_0$  with  $\delta=0.01$



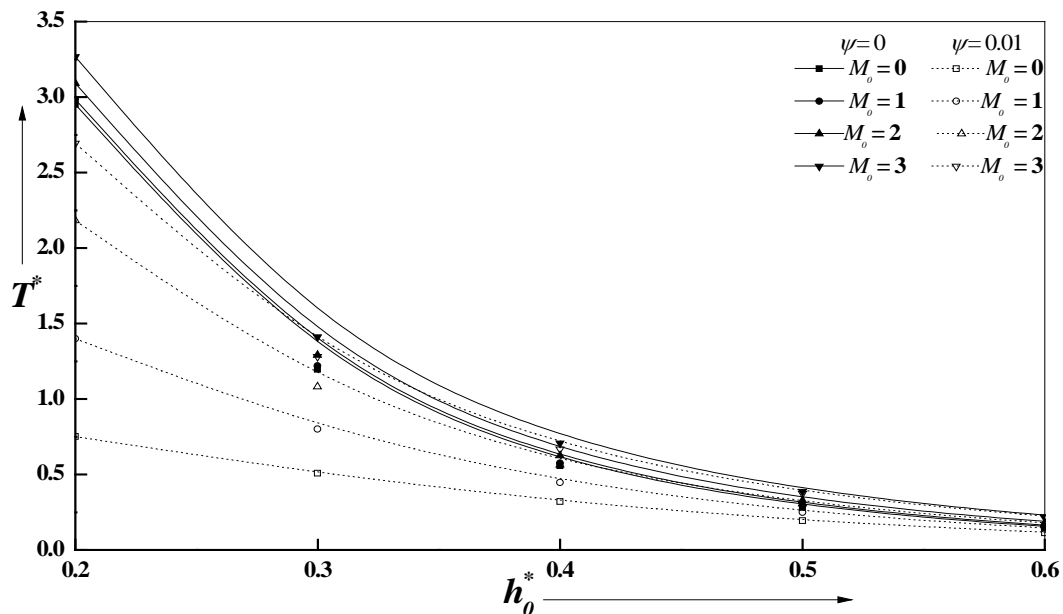


Fig. 6 Variation of non-dimensional  $T$  with  $h_0^*$  for different values of  $\psi$  and  $M_0$  at  $A=0.2$ .

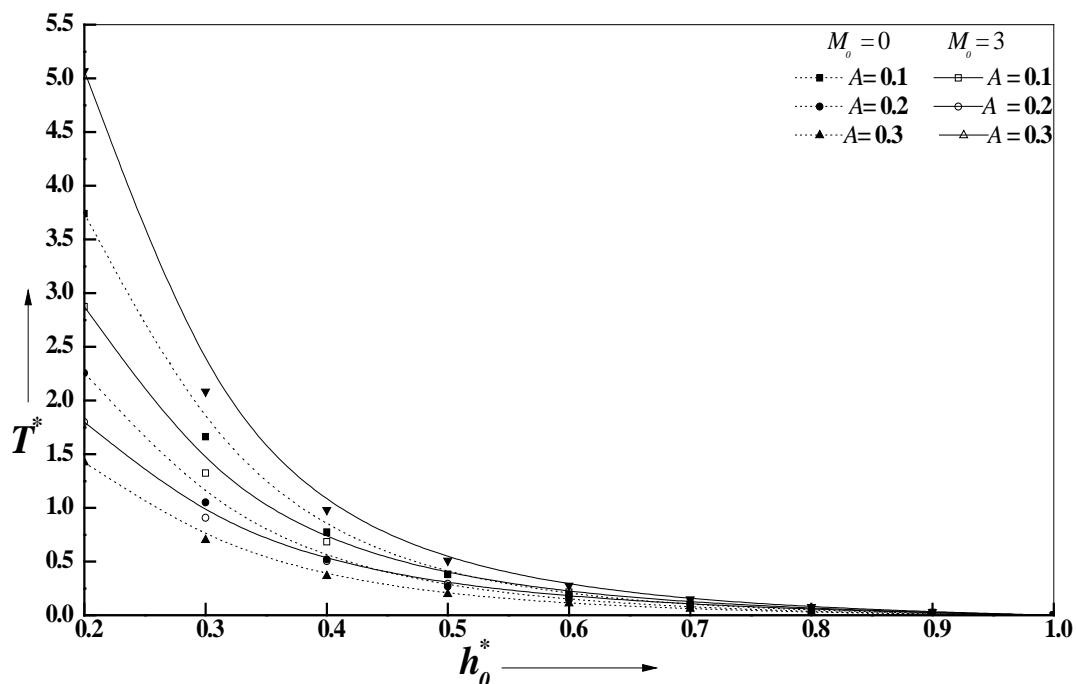
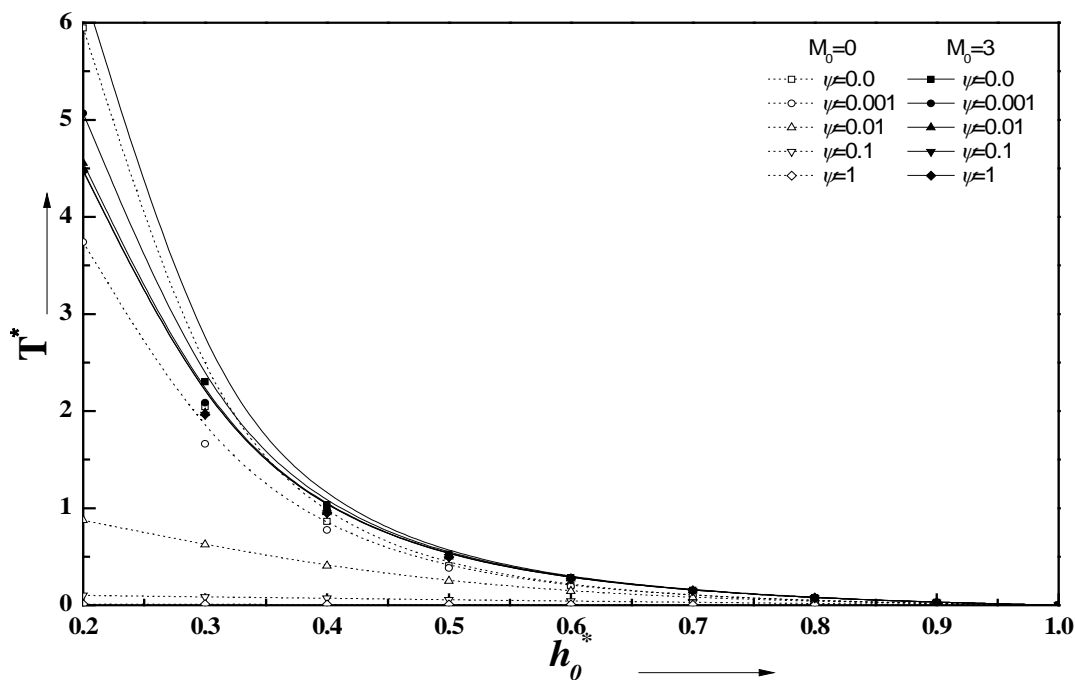


Fig. 7 Variation of non-dimensional  $T^*$  with  $h_0^*$  for different values of  $A$  and  $M_0$  at  $\psi=0.001$ .



**Fig.8** Variation of non-dimensional  $T^*$  with  $h_0^*$  for different values of  $\psi$  and  $M_0$  with  $A=0.1$  and  $\delta=0.01$

**Table-1:** Variation of  $R_{W^*}$  and  $R_{T^*}$  for different values of  $M_0, \psi, \delta = 0.01$  and  $m = 0.6$

		$R_{W^*}$	$R_{T^*}$
$\psi = 0.0$	$M_0 = 1$	18.7857	3.3169
	$M_0 = 2$	74.7225	13.248
	$M_0 = 3$	166.6498	29.753
$\psi = 0.01$	$M_0 = 1$	21.896	35.344
	$M_0 = 2$	81.144	68.878
	$M_0 = 3$	177.246	101.258
$\psi = 1$	$M_0 = 1$	548.387	4644.48
	$M_0 = 2$	873.719	6423.34
	$M_0 = 3$	1391.84	7747

**Source of support: Nil, Conflict of interest: None Declared**

*[Copy right © 2016. This is an Open Access article distributed under the terms of the International Journal of Mathematical Archive (IJMA), which permits unrestricted use, distribution, and reproduction in any medium, provided the original work is properly cited.]*